Utilization of irrigation, drainage, and electrical conductivity data for efficient use of nitrate in a soilless culture system

Tae In Ahn
Korea Institute of Science and Technology
Soo Hyun Park
Korea Institute of Science and Technology
Jung-Seok Yang
Korea Institute of Science and Technology
Ju Young Lee (jyl7318@kist.re.kr)
Korea Institute of Science and Technology https://orcid.org/0000-0002-5531-5523

Research Article

Keywords: Nutrient uptake, Decision support, Fertilizer, Nutrient use efficiency, Nitrogen use efficiency

Posted Date: October 20th, 2020

DOI: https://doi.org/10.21203/rs.3.rs-38941/v2

Utilization of irrigation, drainage, and electrical conductivity data for efficient use of nitrate in a soilless culture system

Tae In Ahn, Soo Hyun Park, Jung-Seok Yang, Ju Young Lee*

Smart Farm Research Center, KIST Gangneung Institute of Natural Products, Gangneung 25451, Republic of Korea

* Corresponding author

Tel: +82-33-650-3703; Fax: +82-33-650-3629; E-mail address: jyl7318@kist.re.kr

Abstract

Nitrate management in agricultural systems has mainly been established based on nitrate supply and the yield response curve. In the case of intensive fertilization systems such as soilless culture, the nitrate amount usually remains above the curve's optimal point. A surplus nutrient supply under these conditions could result in the excessive emission of chemical fertilizers. However, very few studies have developed a decision-making process for the efficient use of nitrate under the soilless culture system online. This study was conducted to develop an indicator related to the absorption of nitrate that can be applied in online systems utilizing the monitored irrigation and drainage amount data, electrical conductivity (EC), and the nitrate analysis data of irrigation and drainage. In the simulation, a stochastic change was generated for the nutrient absorption rate. The cultivation experiment verified the theoretical prediction, and a higher correlation of tomato yield with the nitrate absorption indicator was confirmed than with the nitrate supply amount. Also, the normalization of indicator and tomato yield showed dynamic time-series responses. The simulation and cultivation experiments showed that the indicator related to nitrate absorption estimated by online EC, irrigation, and drainage monitoring provides useful theoretical and experimental frameworks regarding efficient resource management decisions.

Keywords: Nutrient uptake; Decision support; Fertilizer; Nutrient use efficiency; Nitrogen use efficiency

1. Introduction

From the planetary boundaries perspective, the global nitrogen cycle has already transgressed the boundary that humanity can operate safely (Steffen et al., 2015). Along with the growing interest in sustainability, the soilless culture is recently receiving significant attention as one of the promising approaches to manage fertilizers and water by the closed-loop system (Gruda, 2019; Gunton et al., 2016; Pretty et al., 2018). However, unfortunately, most global soilless culture systems on a commercial scale are operated by an open-loop water management system (Massa et al., 2020; Voogt and Bar-Yosef, 2019). Furthermore, the crops grown in substrate systems are cultivated with overall surplus water and nutrients to provide proper root-zone conditions (Sonneveld and Voogt, 2009). In South Korea, 2102 kg of nitrogen fertilizers per ha per year were consumed annually in the open-loop sweet pepper cultivation, and only 5% of soilless production is used for the closed-loop system (Lee and Kim, 2019). Thus, nitrogen emission under intensive fertilizer use practice of the soilless culture system also has been a substantial problem in the field (Massa et al., 2010; Voogt and Bar-Yosef, 2019).

Balancing the yield increase while decreasing nitrogen consumption has long been challenging for sustainable agriculture (Tilman et al., 2002; Zhang et al., 2015). Conventionally, nitrogen management in plant production has mainly been established based on nitrate supply or concentration and the yield response curve. An increase in the supply of nitrogen from a range of deficiencies leads to an increase in yield (Engels et al., 2012). To date, quantitatively summarized nitrogen use and yield response had been used as the primary decision-making process to use appropriate fertilizers (Pan et al., 2020). In an open field agricultural production system, the cultivation fields represent a broad range of plant nutritional conditions, from deficiency to toxicity. However, the yield response curve using the amount of nitrogen supply is only sensitive within the range from deficiency to optimal conditions (Engels et al., 2012). Therefore, under controlled nutrition conditions where nitrogen is managed mostly at moderate or excessive levels, such as in soilless cultures, there are technical difficulties in the online evaluation of efficient nitrogen use (Massa et al., 2011). Therefore, it may be challenging to solve the

nitrogen emission problem in a soilless culture system by conventional nitrogen management practice.

Instead of the nitrogen supply and yield response technique, the nitrogen absorption phenomenon could provide direct information that is more closely related to plant physiological conditions. Also, plant nitrogen uptake changes may include plant growth information such as relative growth rate and vegetative– reproductive growth (Ågren, 2008; Huett, 1996). Thus, the utilization of nitrogen absorption phenomena in the soilless culture system that operates the nitrogen usually above the optimal ranges could expect a more sustainable nitrogen management framework. Significantly, online utilization of the nitrogen absorption could enhance technical applicability. In the controlled experimental conditions such as a single container system, plant nutrient uptake can be accurately calculated (Anpo et al., 2018). Under steady-state and homogeneous conditions, a component's internal process corresponds to the difference between the inputs and outputs (Nordstrom, 2007). However, most soilless culture systems are supplied intermittently with nutrients and irrigation water using an automatic control system (Shin and Son, 2016). Furthermore, in typical soilless culture substrates such as rookwool, a heterogeneous nutrient distribution is formed in the root zone (De Rijck and Schrevens, 1998a). Thus, the soilless culture system has been regarded as too irregular and dynamic for the online estimation of nutrient absorption (Van Noordwijk, 1990).

However, a recent study on the estimation of total nutrient uptake in the soilless culture system has confirmed the possibility of utilizing nutrient absorption indicator in substrate culture conditions through stochastic simulation analyses and normalization of tomato yield data (Ahn et al., 2020). In that study, the stochastic simulation analyses about the dynamic interactions between automated irrigation systems, drainage, electrical conductivity (EC), and transpiration showed that the significant trends in total nutrient absorption could be detected by online data collection of irrigation, drainage, and EC. Even within the total nutrient absorption, an individual nutrient absorption concentration can change dynamically (Van Noordwijk, 1990). However, nitrogen makes up a large proportion of plant nutrition (Steiner, 1980). Also contribute primarily to the EC of nutrient solutions (Savvas and Adamidis, 1999).

Thus, it could be expected that the extended application of these approaches to the utilization of nitrogen absorption information is also feasible.

In the present study, the indicator related to the absorption of nitrate was investigated by the simulation and experimental analyses. The error-provoking conditions, such as intermittent irrigation control, subsequent fluctuations in nutrient concentration, and nonhomogeneous nutrient distribution in the substrate, were simulated. Under these simulated conditions, the nitrate absorption indicator was determined based on irrigation, drainage, EC, and nitrate concentration. The nitrate absorption indicator was applied to the actual soilless culture system to analyze crop yield correlation with the nitrate absorption indicator. In addition, to broaden the range of nitrate absorption of plants, some cultivation experiment lines were subjected to LED inter-lighting conditions.

2. Materials and Methods

2.1 Simulation analysis of nutrient uptake estimation

The model used in the present study simulated the automated nutrient and water management of a soilless culture system in which nutrient absorption, solar radiation, solar radiation-based irrigation control, transpiration, and water content change in the substrate were included (Fig. 1a). The model with cloud cover according to the solar altitude estimation equation was used for the simulation of solar radiation change (Holtslag and Van Ulden, 1983):

$$K^+ = K_0^+\left(1 + b_1 N^{b_2}\right) \quad (1)$$

where, K^+ is the reduced solar radiation by cloud cover; $K_0^+$is the incoming solar radiation at ground level under clear skies, determined by the changes in solar altitude over time and location on the ground; $b_1$and b_2 are the empirical coefficients; and N is the total cloud cover. N is a value between 0 and 1; the closer to 0, the clearer the day and the closer to 1, the cloudier the day. In the simulation analysis, dynamic weather changes were applied using the random-walk process method. In the soilless culture system, the irrigation was controlled based on the integrated solar radiation of $K^+$and it followed the

106 general greenhouse irrigation automation technique (Shin and Son, 2016). Nutrient and water transfers
107 were made by referring to the nutrient transport model under substrate conditions (Silberbush et al.,
108 2005), and the interconnection between the models was based on Ahn and Son's soilless culture system
109 model (Ahn and Son, 2019).

110 For the absorption of nutrients based on the concentration of nutrients in the substrate, the
111 Michaelis-Menten equation was used. The nutrient absorption rate model applies the root surface area
112 reflecting the nutrient absorption capacity of plants:

113 $$J^I = P_{RSA} \frac{J^I_{max}(C^I - C^I_{min})}{K^I_m + (C^I - C^I_{min})} \quad (2)$$

114 where, P_{RSA} is the root surface area (m^2), J^I_{max} (mmol m^{-2} min^{-1}) is the maximum absorption rate of
115 nutrient I, K^I_m (mM) is the Michaelis-Menten constant, and C^I_{min} (mM) is the minimal concentration
116 at which J^I=0. The nutrient elements included in the simulation were K, Ca, Mg, NO_3, and P. In actual
117 soilless culture system, the probability of various outcomes under different environmental conditions
118 could be happened. In this simulation, a stochastic coefficient was applied to the nutrient absorption
119 rate to identify the changes in the rate under various conditions:

120 $$J^I = S_{cof} P_{RSA} \frac{J^I_{max}(C^I - C^I_{min})}{K^I_m + (C^I - C^I_{min})} \quad (3)$$

121 where, S_{cof} is an arbitrary coefficient for applying the multiplication factor to the nutrient absorption
122 rate. In the present study, S_{cof} was used to simulate the stochastic changes in the nutrient absorption
123 rate. S_{cof} corresponds to a random-walk process that increases or decreases with a certain The
124 transpiration model was applied to the empirical version of the Penman–Monteith equation (Bailey et
125 al., 1993; Choi and Shin, 2020):

126 $$Q_{trs} = a\left(1 - e^{-kP_{LAI}P_{VPD}}\right)K^+ + bP_{LAI}P_{VPD} \quad (4)$$

127 where, Q_{trs} is the transpiration rate (L min^{-1}), a and b are the empirical coefficients, k is the
128 extinction coefficient in the plant canopy, P_{LAI} is the leaf area index (LAI), and P_{VPD} is the vapor
129 pressure deficit (VPD). The LAI is a fixed value for the simulation. The tomato leaf area used in the

LAI calculation was estimated by measuring the nondestructive leaf area of the cultivated tomato at the same time as the measured environmental data used for simulation verification (Carmassi et al., 2007). The VPD was simulated to be shifted by the random-walk process between 0.5 and 2.0 kPa to apply the stochastic fluctuation for transpiration. For the simulation of EC based on the nutrient solution supply method, the EC was calculated by an empirical equation for converting the equivalent concentration into EC (Savvas and Adamidis, 1999). Under the simulated conditions, the day nutrient absorption index for total nutrients ($DNAI_{EC}$) and nitrate ($DNAI_{NO3}$) were calculated as the difference between the daily nutrient inflow into the substrate and the outflow from the substrate:

$$DNAI_{EC} = \sum_{i=1}^{n}(EC_i^{Sup} V_i^{Sup} - EC_i^{Drg} V_i^{Drg}) \quad (5)$$

$$DNAI_{NO3} = \sum_{i=1}^{n}(N_i^{Sup} V_i^{Sup} - N_i^{Drg} V_i^{Drg}) \quad (6)$$

where, i and n are day after DNAI calculation and present day, respectively, EC_i^{Sup}, N_i^{Sup}, and V_i^{Sup} are the daily EC (ds/m), nitrate concentration (mM), and volume of the irrigated nutrient solution (L), respectively and EC_i^{Drg}, N_i^{Drg}, and V_i^{Drg} are the daily EC, nitrate concentration, and volume of the drained nutrient solution, respectively. We analyzed the effects of the nutrient absorption rate and drainage ratio in the substrate using simulation analysis and the correlation of $DNAI_{EC}$ (a.u.) and $DNAI_{NO3}$ (mmol) with total nutrient absorption and nitrate absorption, respectively. The main parameters used in this simulation are summarized in Table 1.

2.2 Experimental demonstration of $DNAI_{EC}$ and $DNAI_{NO3}$.

Cultivation experiments were conducted to confirm that the correlation between the predicted $DNAI_{EC, NO3}$ in the simulation and the absorption of plant nutrients was related to the tomato yield in the greenhouse at an experimental farm in the KIST Gangneung (37.8° N, 128.8° E). The experimental crop was tomato and the planting density was 2.67 plants/m^2. The tomato was cultivated on rookwool slabs (Grodan GT Master, Grodan, The Netherlands) with a hanging gutter (9.6 m in length). For the nutrient solution supply, an automatic drip irrigation system using an irrigation method with integrated

154 solar radiation was used. The cultivation area in the greenhouse was 384 m^2, consisting of a total of 18
155 hanging gutters; seven of these were used for $DNAI_{EC}$ and $DNAI_{NO3}$ experiments (Fig. 1). $DNAI_{EC}$ and
156 $DNAI_{NO3}$ were calculated using equations (5) and (6), respectively. The measurement of the nutrient
157 supply and discharge was performed for each hanging gutter. The volume of the daily nutrient solution
158 was measured by installing a digital flow meter (Water Smart Flow Meter, Gardena, Germany)
159 connected to each hanging gutter. For the analysis of NO_3^- of the daily nutrient supply solution, one
160 dripper was placed in a 2 L beaker to measure EC and to collect 50 mL of the nutrient solution after the
161 irrigation stopped. The EC of the daily drainage was measured and 50 mL of the daily drainage was
162 collected after the end of the daily irrigation from the drainage collecting tank (30 × 30 × 50 cm) with
163 an automatic discharge system placed at the drain of the hanging gutter. The drainage volume was
164 measured by reading the water level in the daily drainage tank after the end of irrigation. For NO_3^-
165 analysis, ion chromatography was performed (730 Professional IC, Metrohm, Switzerland). In the
166 experiment, tomatoes were planted on October 8, 2019, and $DNAI_{EC}$ and $DNAI_{NO3}$ measurements were
167 performed from December 31, 2019 (84 days after transplanting, 84 DAT) to January 28, 2020 (112
168 DAT) after planting. To analyze the relationship of tomato yield with $DNAI_{EC}$ and $DNAI_{NO3}$, the total
169 yield of each hanging gutter was periodically measured. Also, to compare the level of vegetative growth
170 of tomato plants, the leaf area was estimated. A non-destructive method was used for the leaf area
171 estimation by measuring leaf width and length (Carmassi et al., 2007).

172 *2.3 Inter-lighting treatments for disturbance application on nutrient absorption*

173 In the present study, inter-lighting was used as a factor that could affect the absorption of nutrients.
174 In tomato cultivation, inter-lighting can affect the production of photosynthetic assimilates, which can
175 be a factor in increasing yield (Tewolde et al., 2016). Thus, the treatment of inter-lighting can have a
176 significant effect on plant growth and nitrate absorption. The treatments consisted of three lines of inter-
177 lighting (Inter1-3) and four lines of control (L1-4) for a total of seven measured hanging gutter lines.

178 The treatment for inter-lighting started on 87 DAT. Inter-lighting performance (LT080, Luco Corp.,
179 Korea) has a photosynthetic photon flux density (PPFD) of 168 μmol m^{-2} s^{-1}, and the distance from the
180 tomato was 10 cm. The inter-lighting irradiation time was adjusted to two experimental conditions. For
181 the first experimental condition, irradiation was applied for 12 h from 22:00 to 10:00 the next day,
182 following the results of tomato inter-lighting by Tewolde et al. (2016). However, after the initial inter-
183 lighting treatment, apparent stress symptoms such as chlorosis and scorch were observed. Therefore,
184 the second light irradiation condition was adjusted on 106 DAT, and the irradiation was conducted for
185 5 h from 17:30 to 22:30. Also, to visualize the dynamic time-series responses, the normalization of the
186 $DNAI_{EC,\ NO3}$ and tomato yield was conducted. The following equation was applied for the normalized
187 transformation:

188 $$x_{nor} = \frac{x - x_{min}}{x_{max} - x_{min}} \quad (7)$$

189 where, x_{nor} is the normalized value, x is the $DNAI_{EC}$, $DNAI_{NO3}$, or the tomato yield to be normalized
190 for each treatment, x_{min} is the smallest $DNAI_{EC}$, $DNAI_{NO3}$, or the tomato yield per treatment, and
191 x_{max} is the largest $DNAI_{EC}$, $DNAI_{NO3}$, or the tomato yield by treatment.
192

193 ## 3. Results

194 ### *3.1 $DNAI_{EC}$ and $DNAI_{NO3}$ in the simulation analysis*

195 By applying the random-walk process to the cloud cover, the simulation results showed a change
196 in the solar radiation and substrate moisture content (Fig. 2a). The changes in nitrate concentration and
197 EC in the substrate were simulated due to the nutrient supply, plant nutrient uptake, and drainage
198 generation based on the water content of the substrate (Fig. 2b and c). In an actual soilless culture system,
199 the probability of various outcomes under different environmental conditions could be happened.
200 Therefore, a stochastic change was applied, and the simulation was replicated with a change in the rate
201 of nutrient absorption from various pathways for nutrient absorption changes (Fig. 2d). Average nutrient

absorption factors of 0.88 and 0.47 were calculated during the simulation iterations, and the changes in the nutrient absorption factor of various distributions between approximately 0.2 and 1.2 were simulated. $DNAI_{EC}$, total nutrient absorption, $DNAI_{NO3}$, nitrate absorption, and the correlation analysis between $DNAI_{EC}$ and $DNAI_{NO3}$ were measured (Fig. 3a–c). $DNAI_{EC}$ and $DNAI_{NO3}$ showed correlations in different ranges depending on the nutrient absorption factors. Specifically, they showed a very high positive correlation. However, the coefficient of determination was higher on the side that had higher nutrient absorption. Based on the average drainage ratio during the simulation period, the $DNAI_{EC, NO3}$-nutrient absorption coefficient of determination showed that the coefficient of determination (R^2) was decreased as the drainage ratio was decreased (Fig. 3d). In addition, the decrease in the R^2 value with a decrease in drainage ratio was greater in the low nutrient uptake magnification distribution.

3.2 Correlation of nitrate supply, concentration, $DNAI_{EC}$, and $DNAI_{NO3}$ with yield in the cultivation experiment

By monitoring during the DNAI calculation period, nitrate supply, average discharged concentration of nitrate, discharge amount, irrigation amount, yield, and partial factor productivity were summarized (Fig. 4). During the experimental period, the cumulative amount of nitrate supplied was relatively slowly increased until 100 DAT. However, a change in the nitrate supply rate was observed over time (Fig. 4a). The nitrate concentration in the drainage decreased during half of the measurement period. However, repetitive trends of increase and decrease were observed over time (Fig. 4b). The discharge amount of nitrate in the drainage was different among treatments (Fig. 4c). Different irrigation amounts were also observed for each treatment, and there was a difference between 262 L (minimum) and 296 L (maximum) (Fig. 4d). The apparent difference was not observed in the cumulative yields and was not different for each treatment during the early stage of DAT; however, it was observed that the deviation increased with increasing DAT (Fig. 4e). A difference in the partial factor productivity of each gutter line was observed from 176 (minimum) to 219 kg yield/kg N use (maximum) (Fig. 4f).

226 The $DNAI_{NO3}$ value slowly increased, similar to the initial nitrate supply amount. In particular, the
227 $DNAI_{NO3}$ value rapidly increased from 95 DAT to 105 DAT (Fig. 5a). However, the deviations between
228 each treatment were large after 105 DAT. $DNAI_{EC}$ showed a similar tendency to that of $DNAI_{NO3}$ (Fig.
229 5b). The R^2 between $DNAI_{EC}$ and $DNAI_{NO3}$ was 0.98, which showed a very high positive correlation.
230 The cumulative nitrate supply amount and tomato yield showed a high level of correlation at 87 DAT
231 and 93 DAT during the initial period of the experiment compared to the other monitoring days (Fig.
232 6a). However, the tendency was different from each other, moving from a positive to a negative
233 correlation. At 87 DAT and 93 DAT, the median positive and median negative relationships were
234 analyzed, respectively. The average nitrate concentration of discharge and yield showed a high level of
235 correlation at 87 DAT and 93 DAT compared to that of the other monitoring days (Fig. 6b). At 87 DAT
236 and 93 DAT, the median negative and median positive relationships were analyzed, respectively.
237 $DNAI_{EC}$ and $DNAI_{NO3}$ had a high negative correlation at 105 DAT and 112 DAT, which was different
238 from the nitrate supply amount and nitrate drainage concentration (Fig. 6c). However, contrary to the
239 yield, the correlation between the non-destructively estimated leaf area and $DNAI_{NO3}$ showed the
240 median positive relationship (Fig. 7).

241 *3.3 Normalized $DNAI_{EC}$, $DNAI_{NO3}$, and tomato yield in the cultivation experiment*

242 The normalized $DNAI_{EC}$ and $DANI_{NO3}$ showed similar trends for each treatment during the
243 experiment (Fig. 8). In particular, the normalized yield of Inter1-3 with inter-lighting decreased after
244 the experimental treatment started. In contrast, the tendency of the normalized $DNAI_{EC}$ and $DNAI_{NO3}$
245 of the Inter1-3 treatment increased after the treatment started. The initial cumulative yield was relatively
246 higher in the L1 gutter line than that of the other lines; however, it decreased to the median level up to
247 100 DAT after which followed a tendency of increasing normalization values of $DNAI_{EC}$ and $DNAI_{NO3}$
248 of L1. The highest cumulative yields were found for the L2 gutter line, except for DAT 87 and DAT
249 100. The normalized $DNAI_{EC}$ and $DNAI_{NO3}$ of L2 were lower at the beginning of the experiment and
250 the higher-level values were monitored at 100 DAT, where a decrease in the normalized yield of L2

was found. The lowest values were observed at 105 DAT and 112 DAT, where high coefficients of determination of $DNAI_{EC}$ and $DNAI_{NO3}$ were analyzed. Overall, the normalized values for yield in the L1, L3, and L4 gutter lines remained high. When they were increased, the $DNAI_{EC}$ and $DANI_{NO3}$ decreased. In addition, when the normalized value for yield was shown to decrease, the $DNAI_{EC}$ and $DNAI_{NO3}$ increased.

4. Discussion

In a conventional soilless culture system, irrigation is stopped at night and commences again after sunrise. Thus, the water content in the substrate is continuously decreased by the VPD at night (Choi and Shin, 2020; Stradiot, 2001). During the day, the rate of transpiration increases due to solar radiation. Daytime irrigation compensates for the transpiration during night and daytime and generates drainage with irrigation exceeding the transpiration rate (Shin and Son, 2016). Therefore, the water content of the medium decreases during the night, then increases in the daytime due to daytime irrigation, with these repeated saturation patterns measured after reaching field capacity (Stradiot, 2001). In the present study, the daily changing pattern in the substrate water content showed that the general moisture management pattern of the soilless culture system was well reflected (Fig. 2a). EC or nutrient concentration in the medium showed dynamic fluctuations due to the nutrient supply, drainage, transpiration, and nutrient uptake (Shin and Son, 2016; Stradiot, 2001; Van Noordwijk, 1990). Fig. 2b and c showed that the daily changing patterns in the variation range of EC and nutrient in the medium were good representations of dynamic fluctuations due to nutrient solution supply, drainage, transpiration, and nutrient absorption. In Fig. 3a and b, $DNAI_{NO3}$ and nitrate absorption had a high positive correlation, as did $DNAI_{EC}$ and total nutrient uptake. Therefore, $DNAI_{EC}$ and $DNAI_{NO3}$ reflect the tendency of nutrient uptake to change with a high probability despite the error-provoking factors in the measurements of the cultivation system. In addition, the coefficient of determination was high when the absorption factor was high compared to the coefficient of determination when the absorption factor

276 was low. At very low drainage, the coefficient of determination was decreased (Fig. 3d). The change in
277 nitrate or total nutrient uptake via $DNAI_{NO3}$ or $DNAI_{EC}$ is difficult to detect during the early stages of
278 growth or when the amount of nutrient absorption is small. Nitrate accounts for a high proportion of the
279 nutrient composition, and the difference in the ratio for several standard compositions is not large (De
280 Rijck and Schrevens, 1998b). Therefore, fluctuations in nitrate can greatly contribute to fluctuations in
281 EC (Massa et al., 2011). In Fig. 3c, the high positive correlation between $DNAI_{EC}$ and $DNAI_{NO3}$ showed
282 that EC is associated with nitrate uptake. The amount of nitrate uptake is very important for the efficient
283 management of nitrate (Massa et al., 2011). However, there are practical limitations in measuring the
284 amount of nitrate absorption in a cultivation system and using it for cultivation management. In a
285 soilless culture system, the use of efficient nitrogen management technology required the prediction
286 model of the absorption of nutrients or the experimental evaluation of the average nutrient absorption
287 concentration from via preliminary investigation of crops (Magán et al., 2005; Massa et al., 2011; Van
288 Noordwijk, 1990). These simulation results provide reliable information on total nutrient and nitrogen
289 absorption via the accumulated $DNAI_{EC}$ and $DNAI_{NO3}$ values under normal cultivation conditions. In
290 addition, the relationship between plant production and $DNAI_{EC}$ or $DNAI_{NO3}$ has implications in terms
291 of providing decision-making tools for the optimization of resource utilization.

292 During the cultivation experiment in the present study, a maximum deviation of 36 L was observed
293 for the cumulative irrigation between the gutter line of each treatment, which affected the difference in
294 the cumulative supply of nitrate (Fig. 4a and d). It was confirmed that the difference in the partial factor
295 productivity was up to 43 kg yield/kg N via moderate deviation between the gutter line of each treatment
296 (Fig. 4f). However, the difference in the amount of nitrate supplied in each gutter line did not show a
297 high correlation with the final yield and there was no consistent trend (Fig. 5a). The average nitrate
298 concentration in drainage shows the nitrate concentration in the root zone, which is also important index
299 for nitrogen-crop yield management (Xiong et al., 2017); however, it did not show a high correlation in
300 the present study (Fig. 6b). The relationship between the supply of nitrogen fertilizer in a previous study

and the increase in production is seen in the low supply range starting from deficiency (Engels et al., 2012). However, if the fertilization amount is increased to a certain level, a diminishing return is observed under the relationship between fertilizer supply and yield response (Tilman et al., 2002). In the area of a diminishing return, there is no significant response to the supply of fertilizer. In the soilless culture system, nitrogen is generally managed under a moderate or excessive range. Therefore, efficient nitrogen management based on fertilizer supply is difficult in soilless cultures. In these areas, actual nutrient absorption might be a more direct indicator than the fertilizer supply rate.

In this experiment, $DNAI_{EC}$ and $DNAI_{NO3}$ showed a high negative correlation with a cumulative yield at DAT 105 and DAT 112 (Fig. 6c). The balance of tomato vegetative and reproductive growth has an important effect on fruit yield. Tomatoes can be biased to vegetative growth when nitrogen is absorbed excessively, which can lead to a decrease in yield (Sainju et al., 2003). In this cultivation experiment, the analyzed $DNAI_{NO3}$ and yield showed a negative correlation. In contrast to the $DNAI_{NO3}$ and yield relationship, leaf area and $DNAI_{NO3}$ showed a positive correlation (Fig. 7), and this could be attributed to the balanced growth of tomatoes. For the nutrient absorption phenomenon, nutrients are also stored in vacuoles in addition to the structure of the plant to maintain ionic homeostasis (Amtmann and Leigh, 2009). However, from a plant stoichiometric point of view, nutrient accumulation dominantly contributes to the growth of the plant structure and has a high relationship with the relative growth rate (Ågren, 2008). In the present study, $DNAI_{EC}$ and $DNAI_{NO3}$ showed a high correlation with cumulative yield compared to nitrate supply or nitrate concentration, which is a traditional indicator of agronomic resource management. This was presumed to be based on the result reflecting the change in the absorption amount based on the plant growth state of each treatment. The point at which a high determination coefficient was observed was the period during which the drainage ratio was increased (Fig. 6c), and these results were consistent with the simulation results (Fig. 3d). The difference in tomato production for each treatment is shown as a result of the difference in the micro-environment of each cultivation space and plant growth status according to the micro-environment of each cultivation space.

In the present study, inter-lighting was applied to some gutter lines to change the growth and absorption of nutrients by creating additional disturbances in the micro-environment compared to the control treatment. Data normalization was performed to analyze the relative changes in yield, $DNAI_{EC}$, and $DNAI_{NO3}$ between each treatment during the experimental period. Overall, $DNAI_{EC}$ and $DNIA_{NO3}$ increased when the normalized value of the yield decreased. In particular, in Inter1-3, the value of the normalization of the yields after treatment decreased simultaneously and a simultaneous increase in $DNAI_{EC}$ and $DNAI_{NO3}$ was observed (Fig. 8). Nitrate and the light environment of plants are in a physiologically close relationship (Lillo and Appenroth, 2001). The relationship between light and nitrate uptake is already well-known and there is an experimental case reporting nitrate uptake increases in LED supplemental lighting treatment (Wojciechowska et al., 2016). Even though in the present study, the LED inter-lighting treatment application showed light stress symptoms, it was found that the increase of the normalized $DNAI_{NO3}$ in the inter-lighting treatment was prominent (Fig. 8). Similar trends were observed in $DNAI_{EC}$, which showed changes in the total nutrient absorption in the simulation.

From a conventional agronomical point of view, the relationship between nitrogen fertilizers and plant production can be defined primarily as an increase in plant yield with increasing fertilizer supply (Pan et al., 2020; Tilman et al., 2002). In the soilless culture system, nitrate generally remains within a moderate or excessive range. Thus, nitrate in these ranges can often be managed in excess. However, this study's theoretical and experimental results provide a technical framework to utilize nitrate absorption indicators in the soilless culture system online.

5. Conclusions

The present study showed that in systems where intensive nitrate management is administered, such as soilless culture systems, nitrogen management based on nitrate supply or concentration might have some restrictions in proper resource management. $DNAI_{EC}$ and $DNAI_{NO3}$ also showed a high positive correlation, and thus are expected to improve the technological ease of applying the $DNAI_{NO3}$

in the system online. Furthermore, the normalized $DNAI_{NO3}$ responded to changes in the normalized yield for each gutter line treatment during the cultivation period based on the relatively high correlation. The time-series response of the normalized $DNAI_{NO3}$ shows potential usability as an onsite decision-support technique for efficient yield-promoting nitrate management. Although this study may be limited in variations of crops and growing media verification, these approaches are expected to provide a technical framework to utilize nitrogen absorption indicators in the soilless culture system online for sustainable resource management.

Abbreviations

DNAI: day nutrient absorption index; EC: electrical conductivity, PPFD: photosynthetic photon flux density, DAT: days after transplanting; VPD: vapor pressure deficit; LAI: leaf area index.

Declaration of Competing Interest

The authors report no declarations of interest.

Acknowledgements

This work was supported by Korea Institute of Planning and Evaluation for Technology in Food, Agriculture and Forestry (IPET) through Smart Plant Farming Industry Technology Development Program, funded by Ministry of Agriculture, Food and Rural Affairs (MAFRA) (No. 119091-01-1-SB020) and by National R&D Program through the National Research Foundation of Korea (NRF) funded by Ministry of Science and ICT (2020M3A9I3037807) (Projecr No. 1711119185).

References

Ågren, G.I., 2008. Stoichiometry and nutrition of plant growth in natural communities. Annu. Rev. Ecol. Evol. Syst. 39, 153–170. https://doi.org/10.1146/annurev.ecolsys.39.110707.173515

Ahn, T.I., Son, J.E., 2019. Theoretical and experimental analysis of nutrient variations in electrical conductivity-based closed-loop soilless culture systems by nutrient replenishment method. Agronomy 9, 649. https://doi.org/10.3390/agronomy9100649

Ahn, T.I., Yang, J.-S., Park, S.H., Moon, H.W., Lee, J.Y., 2020. Translation of irrigation, drainage, and electrical conductivity data in a soilless culture system into plant growth information for the development of an online indicator related to plant nutritional aspects. Agronomy 10, 1306. https://doi.org/10.3390/agronomy10091306

Amtmann, A., Leigh, R., 2009. Ion homeostasis, in: Pareek, A., Sopory, S.K., Bohnert, H.J. (Eds.), Abiotic Stress Adaptation in Plants. Springer Netherlands, Dordrecht, pp. 245–262.

Anpo, M., Fukuda, H., Wada, T., 2018. Plant factory using artificial light: adapting to environmental disruption and clues to agricultural innovation, 1st ed. Elsevier Science, Amsterdam.

Bailey, B.J., Montero, J.I., Biel, C., Wilkinson, D.J., Anton, A., Jolliet, O., 1993. Transpiration of *Ficus benjamina*: comparison of measurements with predictions of the Penman-Monteith model and a simplified version. Agric. For. Meteorol. 65, 229–243. https://doi.org/10.1016/0168-1923(93)90006-4

Carmassi, G., Incrocci, L., Incrocci, G., Pardossi, A., 2007. Non-destructive estimation of leaf area in tomato (*Solanum lycopersicum* L.) and gerbera (*Gerbera jamesonii* H. Bolus). Agric. Mediterr. 137, 172–176.

Choi, Y.B., Shin, J.H., 2020. Development of a transpiration model for precise irrigation control in tomato cultivation. Sci. Hortic. 267, 109358. https://doi.org/10.1016/j.scienta.2020.109358

De Rijck, G., Schrevens, E., 1998a. Distribution of nutrients and water in rockwool slabs. Sci. Hortic. 72, 277–285. https://doi.org/10.1016/s0304-4238(97)00144-1

De Rijck, G., Schrevens, E., 1998b. Comparison of the mineral composition of twelve standard

nutrient solutions. J. Plant Nutr. 21, 2115–2125. https://doi.org/10.1080/01904169809365548

Engels, C., Kirkby, E., White, P., 2012. Mineral nutrition, yield and source–sink relationships, in: Marschner, H., Marschner, P. (Eds.), Marschner's Mineral Nutrition of Higher Plants. Elsevier, Waltham, pp. 85–133.

Holtslag, A.A.M., Van Ulden, A.P., 1983. A simple scheme for daytime estimates of the surface fluxes from routine weather data. J. Climate Appl. Meteor. 22, 517–529. https://doi.org/10.1175/1520-0450(1983)022<0517:ASSFDE>2.0.CO;2

Huett, D.O., 1996. Prospects for manipulating the vegetative-reproductive balance in horticultural crops through nitrogen nutrition: a review. Aust. J. Agric. Res. 47, 47–66. https://doi.org/10.1071/ar9960047

Kim, W.S., Lieth, J.H., 2012. Simulation of year-round plant growth and nutrient uptake in Rosa hybrida over flowering cycles. Hortic. Environ. Biotechnol. 53, 193–203. https://doi.org/10.1007/s13580-012-0054-y

Lillo, C., Appenroth, K.-J., 2001. Light regulation of nitrate reductase in higher plants: which photoreceptors are involved? Plant Biol. 3, 455–465. https://doi.org/10.1055/s-2001-17732

Magán, J.J., Casas, E., Gallardo, M., Thompson, R.B., Lorenzo, P., 2005. Uptake concentrations of a tomato crop in different salinity conditions. Acta Hortic. 365–369. https://doi.org/10.17660/ActaHortic.2005.697.46

Massa, D., Incrocci, L., Maggini, R., Bibbiani, C., Carmassi, G., Malorgio, F., Pardossi, A., 2011. Simulation of crop water and mineral relations in greenhouse soilless culture. Environ. Modell. Softw. 26, 711–722. https://doi.org/10.1016/j.envsoft.2011.01.004

Massa, D., Incrocci, L., Maggini, R., Carmassi, G., Campiotti, C.A., Pardossi, A., 2010. Strategies to decrease water drainage and nitrate emission from soilless cultures of greenhouse tomato. Agric. Water Manag. 97, 971–980. https://doi.org/10.1016/j.agwat.2010.01.029

Massa, D., Magán, J.J., Montesano, F.F., Tzortzakis, N., 2020. Minimizing water and nutrient

losses from soilless cropping in southern Europe. Agric. Water Manag. 241, 106395. https://doi.org/10.1016/j.agwat.2020.106395

Nordstrom, D.K., 2007. 5.02 - Modeling Low-Temperature Geochemical Processes, in: Holland, H.D., Turekian, K.K. (Eds.), Treatise on Geochemistry. Pergamon, Oxford, pp. 1–38. https://doi.org/10.1016/B0-08-043751-6/05074-X

Pan, W.L., Kidwell, K.K., McCracken, V.A., Bolton, R.P., Allen, M., 2020. Economically optimal wheat yield, protein and nitrogen use component responses to varying N supply and genotype. Front. Plant Sci. 10, 1790. https://doi.org/10.3389/fpls.2019.01790

Sainju, U., Dris, R., Singh, B., 2003. Mineral nutrition of tomato. Food Agric. Environ. 1, 176–183.

Savvas, D., Adamidis, K., 1999. Automated management of nutrient solutions based on target electrical conductivity, pH, and nutrient concentration ratios. J. Plant Nutr. 22, 1415–1432. https://doi.org/10.1080/01904169909365723

Shin, J.H., Son, J.E., 2016. Application of a modified irrigation method using compensated radiation integral, substrate moisture content, and electrical conductivity for soilless cultures of paprika. Sci. Hortic. 198, 170–175. https://doi.org/10.1016/j.scienta.2015.11.015

Silberbush, M., Ben-Asher, J., 2001. Simulation study of nutrient uptake by plants from soilless cultures as affected by salinity buildup and transpiration. Plant Soil 233, 59–69. https://doi.org/10.1023/A:1010382321883

Silberbush, M., Ben-Asher, J., Ephrath, J.E., 2005. A model for nutrient and water flow and their uptake by plants grown in a soilless culture. Plant Soil 271, 309–319. https://doi.org/10.1007/s11104-004-3093-z

Sonneveld, C., Voogt, W., 2009. Plant nutrition of greenhouse crops. Springer, Dordrecht ; New York.

Steffen, W., Richardson, K., Rockström, J., Cornell, S.E., Fetzer, I., Bennett, E.M., Biggs, R.,

446 Carpenter, S.R., de Vries, W., de Wit, C.A., Folke, C., Gerten, D., Heinke, J., Mace, G.M., Persson,
447 L.M., Ramanathan, V., Reyers, B., Sörlin, S., 2015. Planetary boundaries: Guiding human development
448 on a changing planet. Science 347. https://doi.org/10.1126/science.1259855
449 Steiner, A.A., 1980. The selective capacity of plants for ions and its importance for the composition
450 and treatment of the nutrient solution. Acta Hortic. 98, 87–97.
451 Stradiot, P., 2001. The grodan water content meter for root management in stonewool. Acta Hortic.
452 71–78. https://doi.org/10.17660/ActaHortic.2001.548.6
453 Tewolde, F.T., Lu, N., Shiina, K., Maruo, T., Takagaki, M., Kozai, T., Yamori, W., 2016. Nighttime
454 supplemental LED inter-lighting improves growth and yield of single-truss tomatoes by enhancing
455 photosynthesis in both winter and summer. Front. Plant Sci. 7. https://doi.org/10.3389/fpls.2016.00448
456 Tilman, D., Cassman, K.G., Matson, P.A., Naylor, R., Polasky, S., 2002. Agricultural sustainability
457 and intensive production practices. Nature 418, 671–677. https://doi.org/10.1038/nature01014
458 Van Noordwijk, M., 1990. Synchronisation of supply and demand is necessary to increase
459 efficiency of nutrient use in soilless horticulture, in: van Beusichem, M.L. (Ed.), Plant Nutrition —
460 Physiology and Applications: Proceedings of the Eleventh International Plant Nutrition Colloquium, 30
461 July–4 August 1989, Wageningen, The Netherlands. Springer Netherlands, Dordrecht, pp. 525–531.
462 Voogt, W., Bar-Yosef, B., 2019. Chapter 10 - Water and Nutrient Management and Crops Response
463 to Nutrient Solution Recycling in Soilless Growing Systems in Greenhouses, in: Raviv, M., Lieth, J.H.,
464 Bar-Tal, A. (Eds.), Soilless Culture (Second Edition). Elsevier, Boston, pp. 425–507.
465 https://doi.org/10.1016/B978-0-444-63696-6.00010-4
466 Wojciechowska, R., Kołton, A., Długosz-Grochowska, O., Knop, E., 2016. Nitrate content in
467 Valerianella locusta L. plants is affected by supplemental LED lighting. Sci. Hortic. 211, 179–186.
468 https://doi.org/10.1016/j.scienta.2016.08.021
469 Xiong, J., Tian, Y., Wang, J., Liu, W., Chen, Q., 2017. Comparison of coconut coir, rockwool, and
470 peat cultivations for tomato production: nutrient balance, plant growth and fruit quality. Front. Plant

471 Sci. 8, 1327. https://doi.org/10.3389/fpls.2017.01327
472 Zhang, X., Davidson, E.A., Mauzerall, D.L., Searchinger, T.D., Dumas, P., Shen, Y., 2015.
473 Managing nitrogen for sustainable development. Nature 528, 51–59.
474 https://doi.org/10.1038/nature15743
475

476 **Table 1** Parameters used for the simulations of the soilless culture system.

Symbol	Description	Value	Reference
P_{LAI}	Leaf area index	7.4	Measured in this study
a	Transpiration empirical parameter	0.588	Shin and Choi (2020)
b	Transpiration empirical parameter	9.092	
k	Extinction coefficient	0.84	
J_{max}^{K}	Maximum absorption rate	0.009	Kim and Lieth (2012)
J_{max}^{Ca}	Maximum absorption rate	0.003	
$J_{max}^{NO_3}$	Maximum absorption rate	0.012	
J_{max}^{P}	Maximum absorption rate	0.002	
K_m^K	Michaelis-Menten constant	3.185	
K_m^{Ca}	Michaelis-Menten constant	0.617	
K_m^{Mg}	Michaelis-Menten constant	0.252	
$K_m^{NO_3}$	Michaelis-Menten constant	4.432	
K_m^P	Michaelis-Menten constant	0.358	
C_{min}^{K}	Minimal concentration for uptake	0.002	
C_{min}^{Ca}	Minimal concentration for uptake	0.002	
C_{min}^{Mg}	Minimal concentration for uptake	0.002	

$C_{min}^{NO_3}$	Minimal concentration for uptake	0.002	
C_{min}^{P}	Minimal concentration for uptake	0.002	
P_{RSA}	Root surface area	0.75	Silberbush et al., (2005); Silberbush and Ben-Asher (2001)

477

478

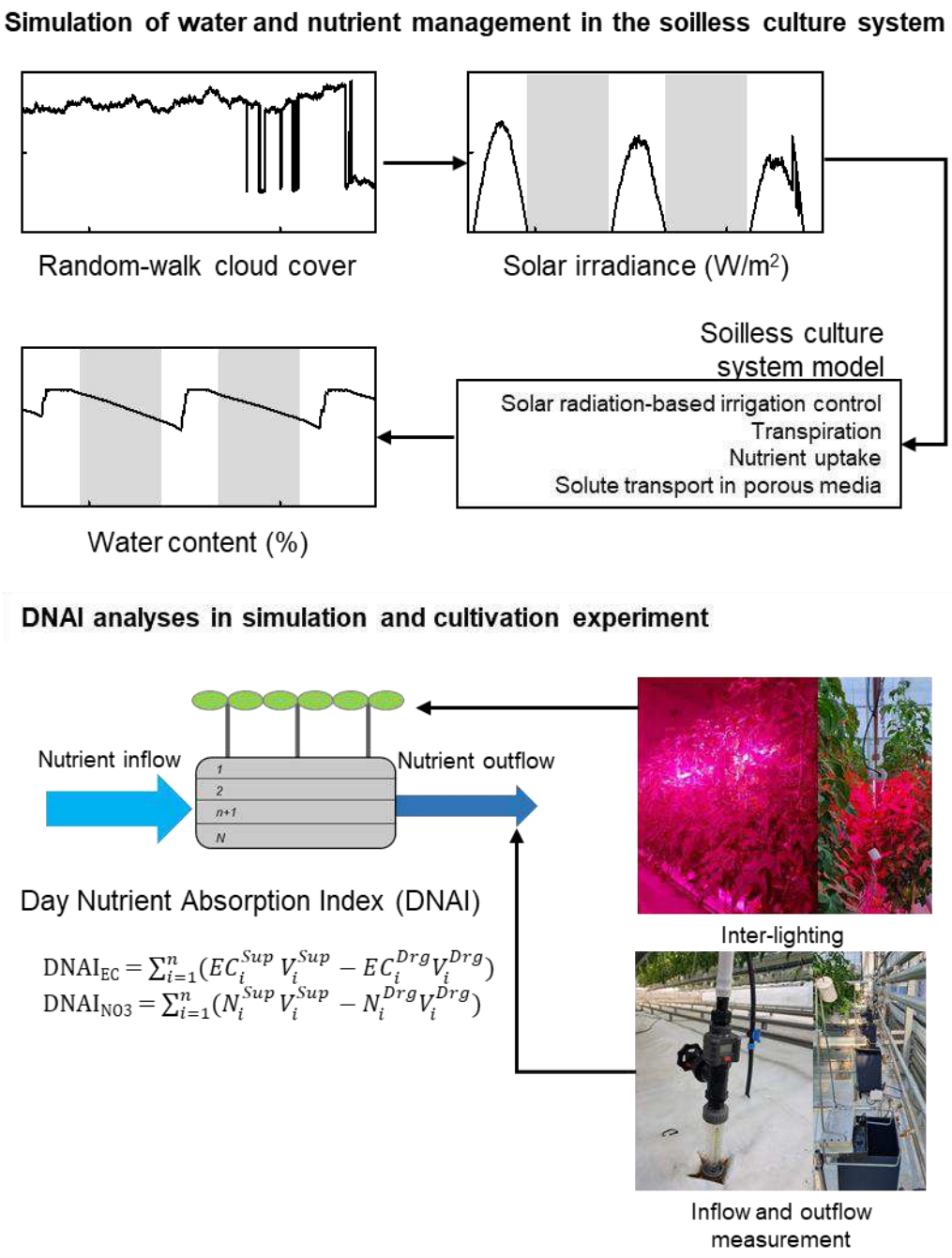

Fig. 1 Schematic diagram of the simulation and experimental analysis.

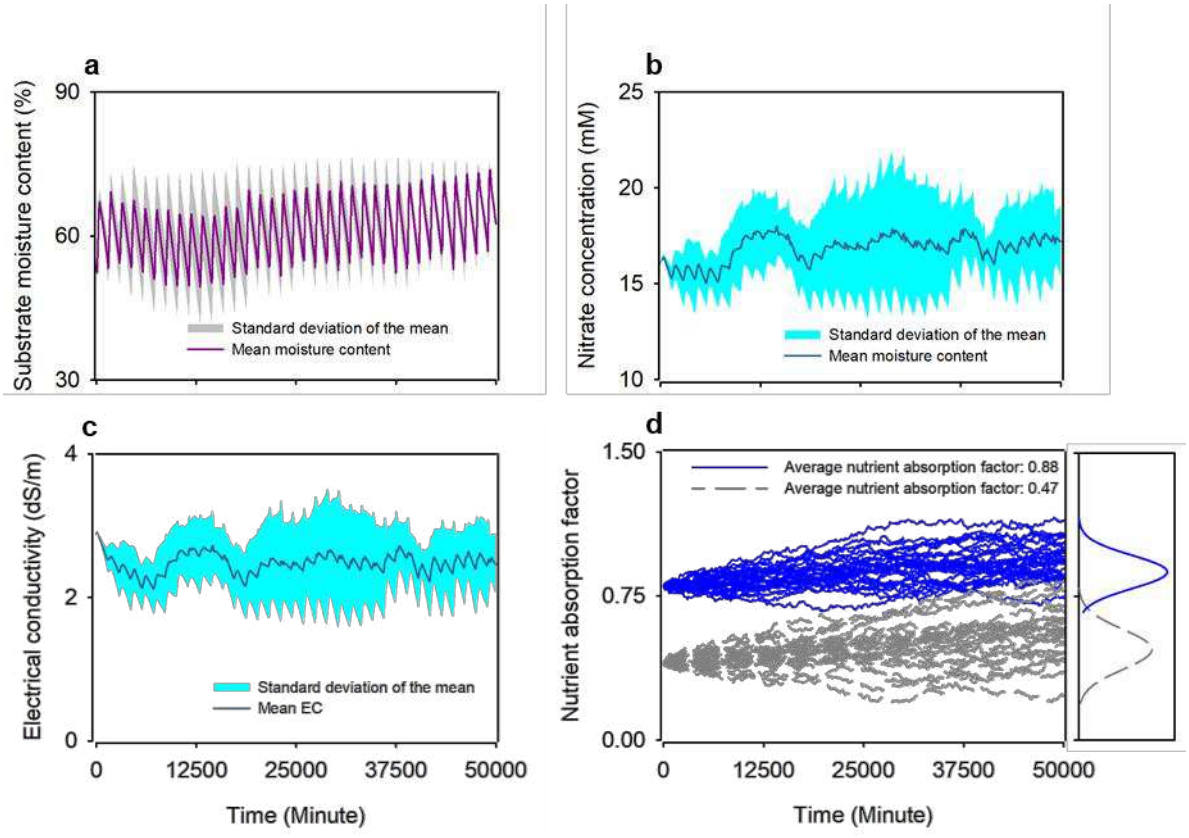

482

483 **Fig. 2** Stochastic changes in substrate moisture content (a), nitrate concentration (b), electrical

484 conductivity (EC, b), and nutrient absorption factor (d) in the soilless culture system simulation.

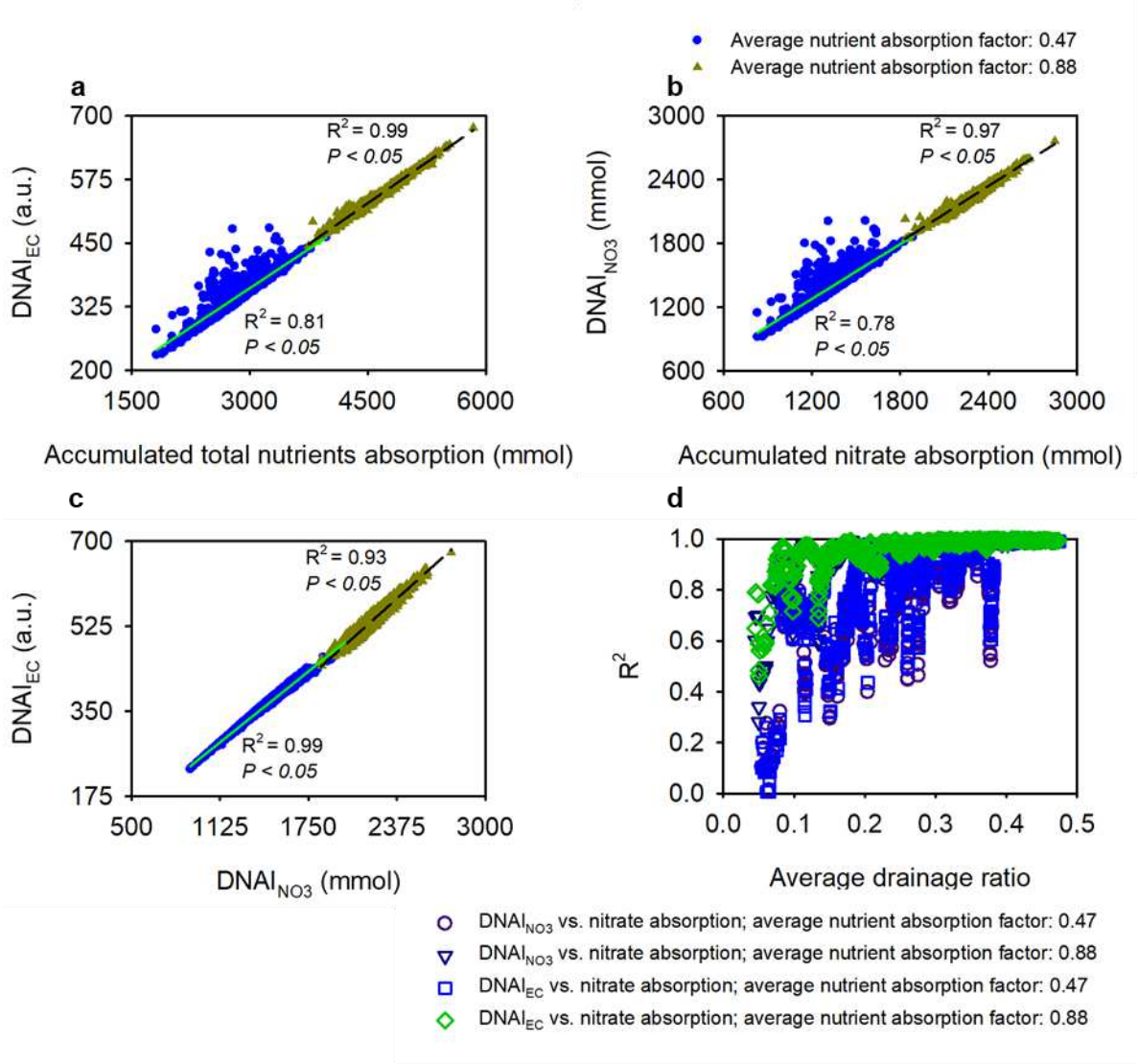

485

486 **Fig. 3** Correlations of $DNAI_{EC}$ (a) and $DNAI_{NO3}$ (b) with total nutrients and nitrate absorption under
487 different average nutrient absorption factors in the simulation; (c) correlations between $DNAI_{EC}$ and
488 $DNAI_{NO3}$ under different average nutrient absorption factors in the simulation; (d) changes in R^2
489 between $DNAI_{EC, NO3}$ and total nutrient or nitrate absorption according to average drainage ratio in the
490 simulation (Number of simulations: 1000).

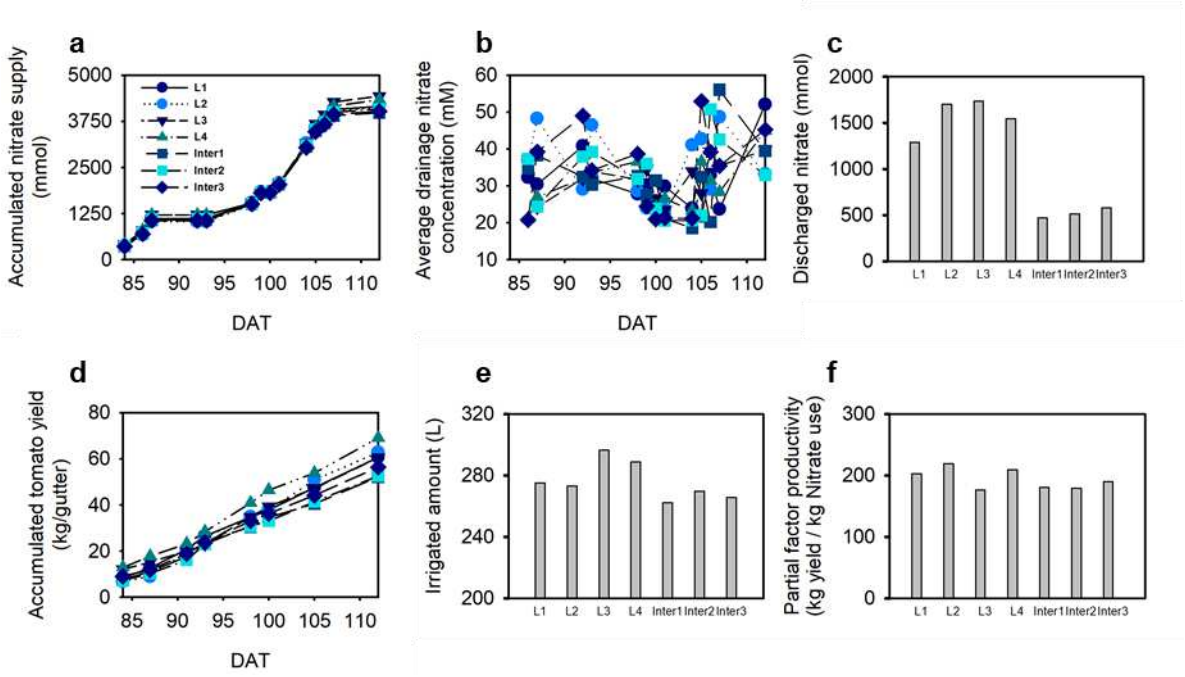

Fig. 4 Accumulated nitrate supply (a), average nitrate concentration in drainage (b), accumulated discharged amount of nitrate (c), accumulated irrigation amount (d), accumulated tomato yield (e), and partial factor productivity (f) during the experimental period.

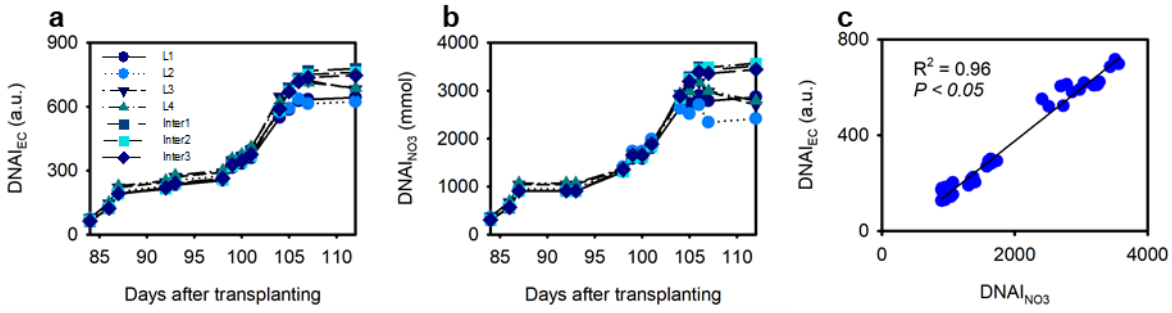

Fig. 5 Changes in $DNAI_{EC}$ (a) and $DNAI_{NO3}$ (b) during the experimental period; (c) correlation between $DNAI_{EC}$ and $DNAI_{NO3}$.

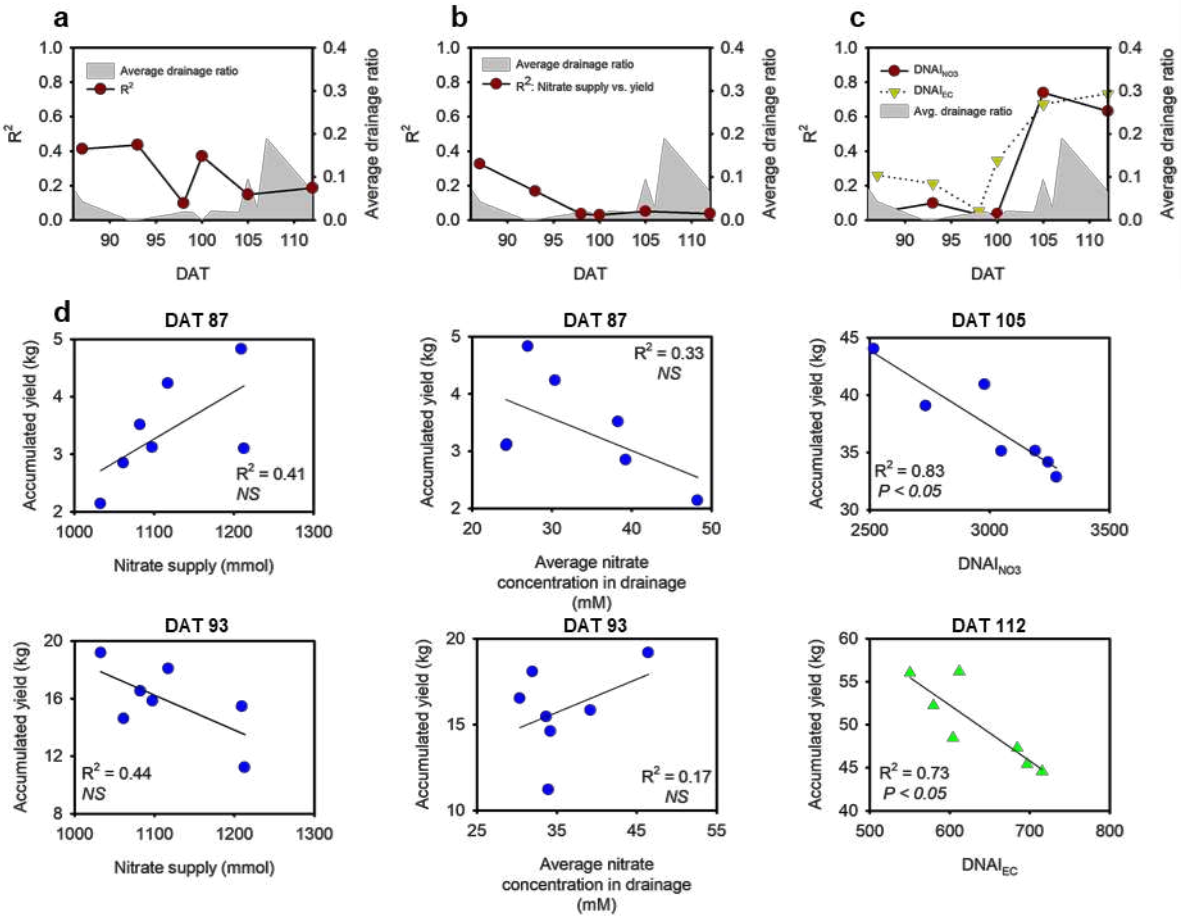

498

499 **Fig. 6** Changes in R^2 values of the accumulated tomato yield with accumulated nitrate supply (a),
500 average nitrate concentration in drainage (b), $DNAI_{EC}$ (c), and $DNAI_{NO3}$ (c); (d) representative
501 correlations of accumulated tomato yield with accumulated nitrate supply, average nitrate concentration
502 in drainage, $DNAI_{EC}$, and $DNAI_{NO3}$.

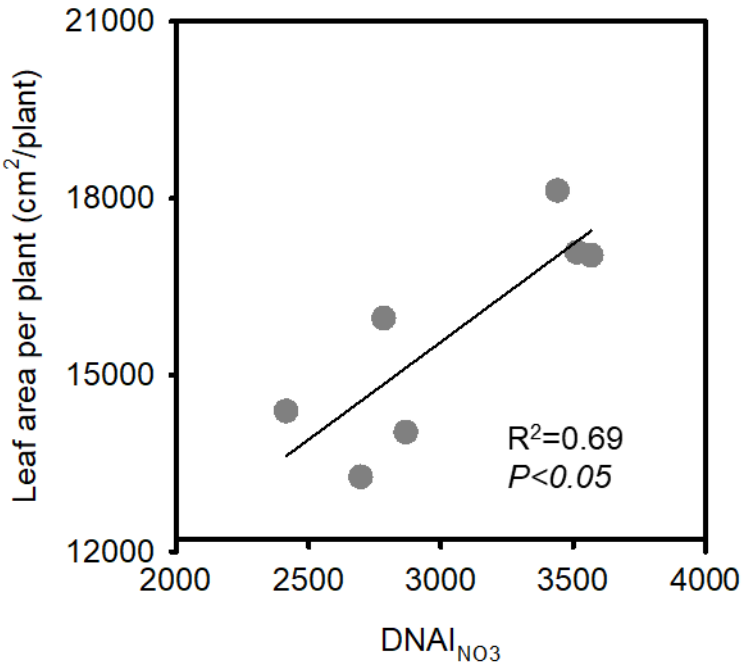

503

504 **Fig. 7** Correlation between non-destructively estimated tomato leaf area and $DNAI_{NO3}$ at the end

505 of the experiment.

506

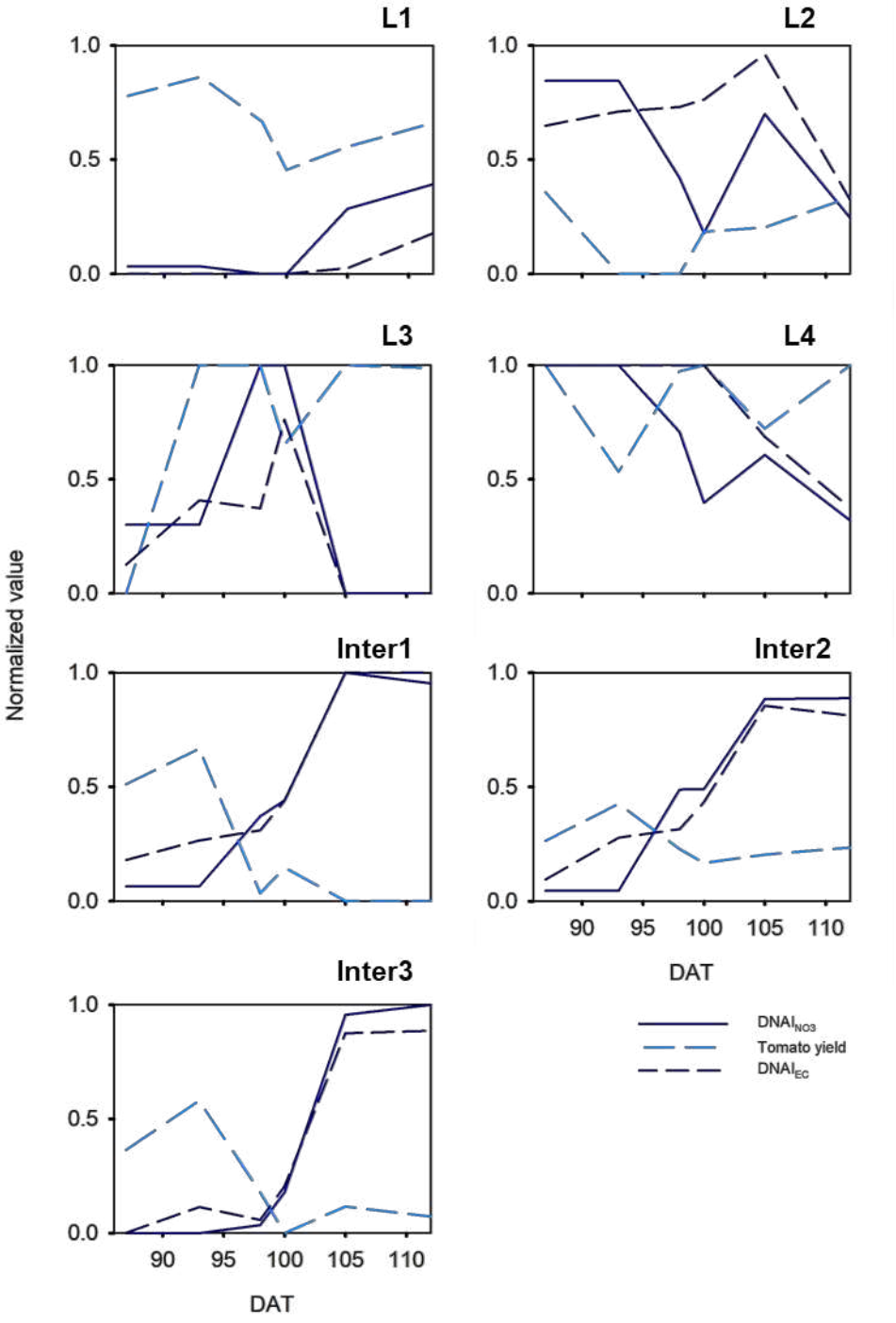

507

508 **Fig. 8** Changes in the normalized values of $DNAI_{EC}$, $DNAI_{NO3}$, and accumulated tomato yield

509 during the experimental period.

510

Figures

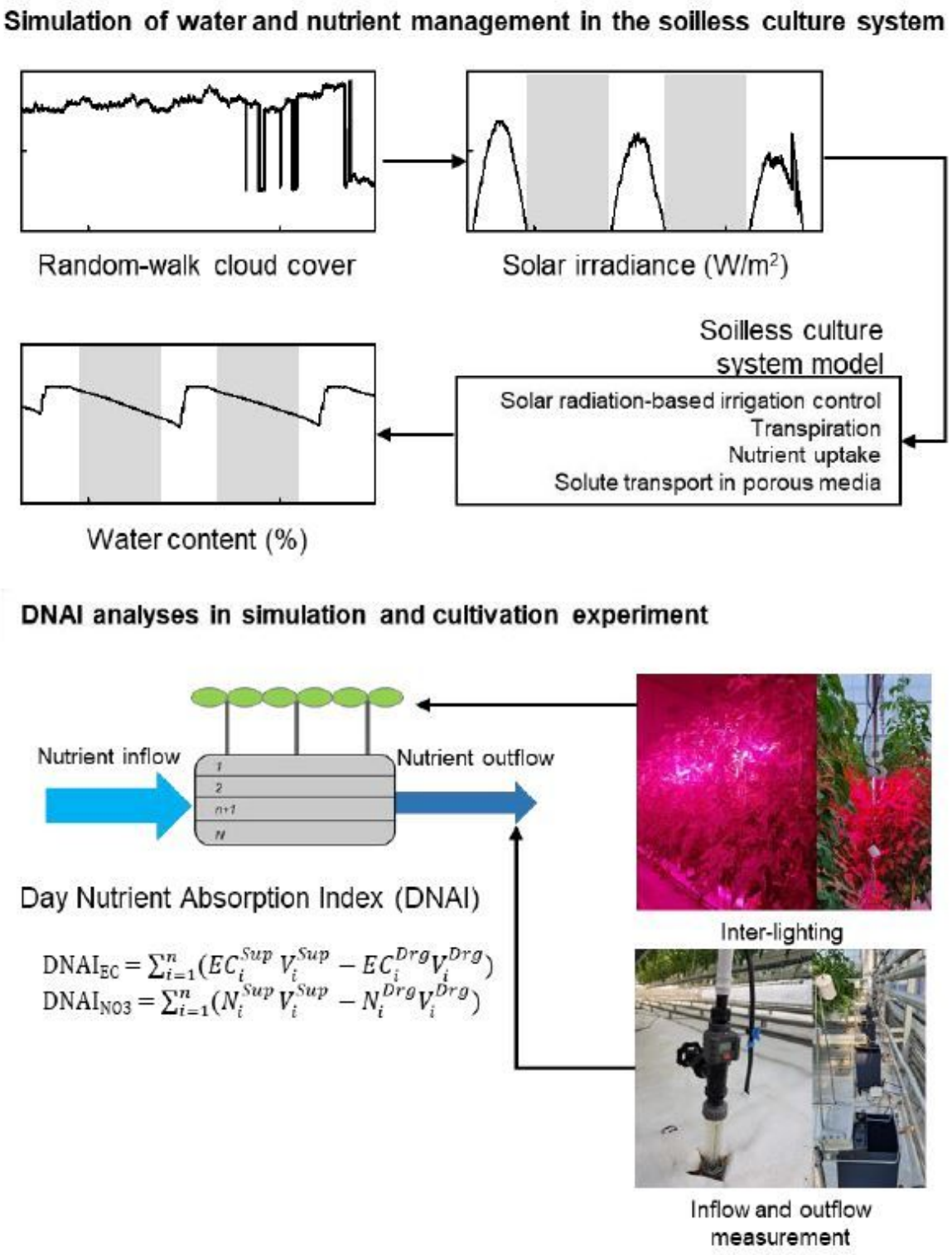

Figure 1

Schematic diagram of the simulation and experimental analysis.

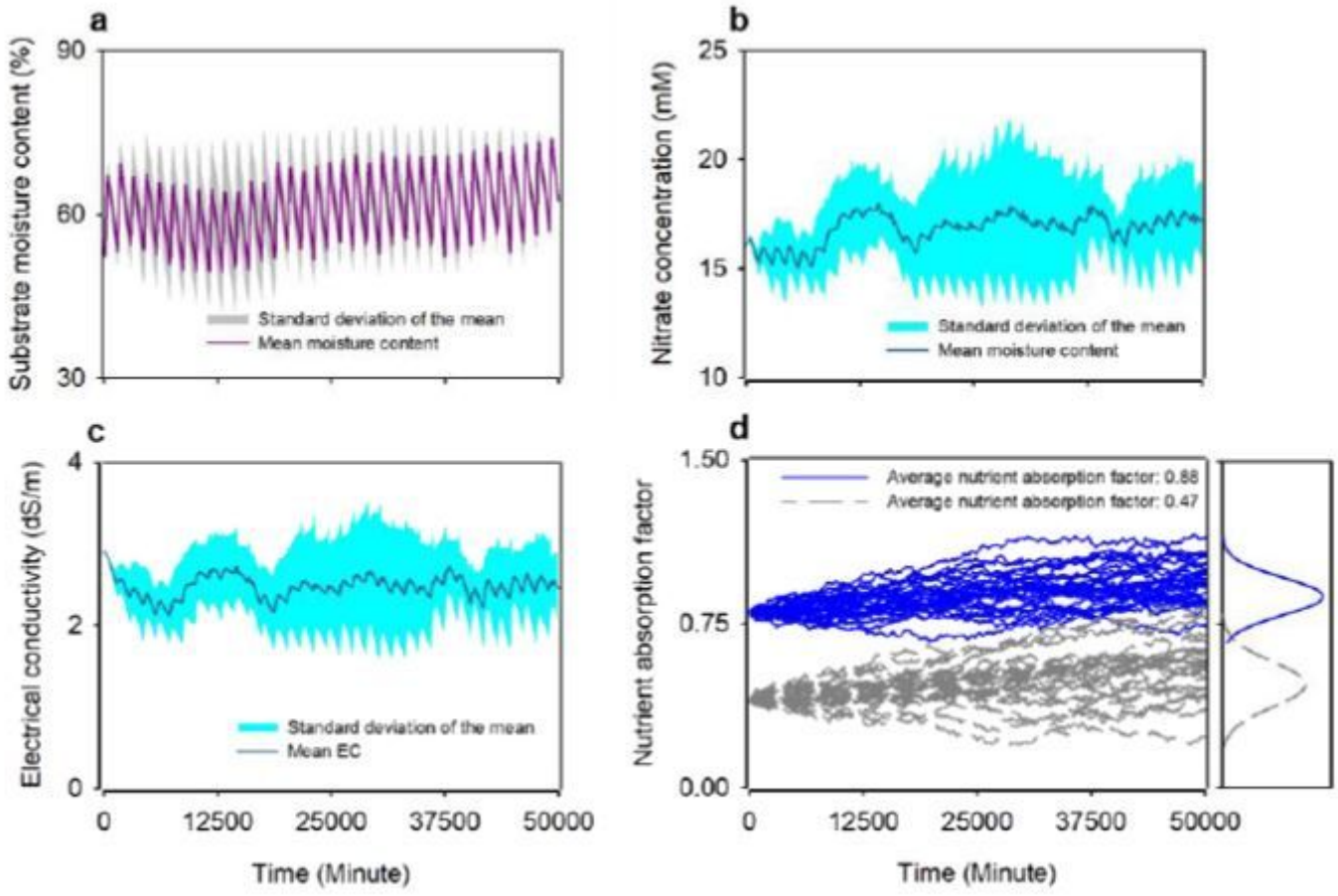

Figure 2

Stochastic changes in substrate moisture content (a), nitrate concentration (b), electrical conductivity (EC, b), and nutrient absorption factor (d) in the soilless culture system simulation.

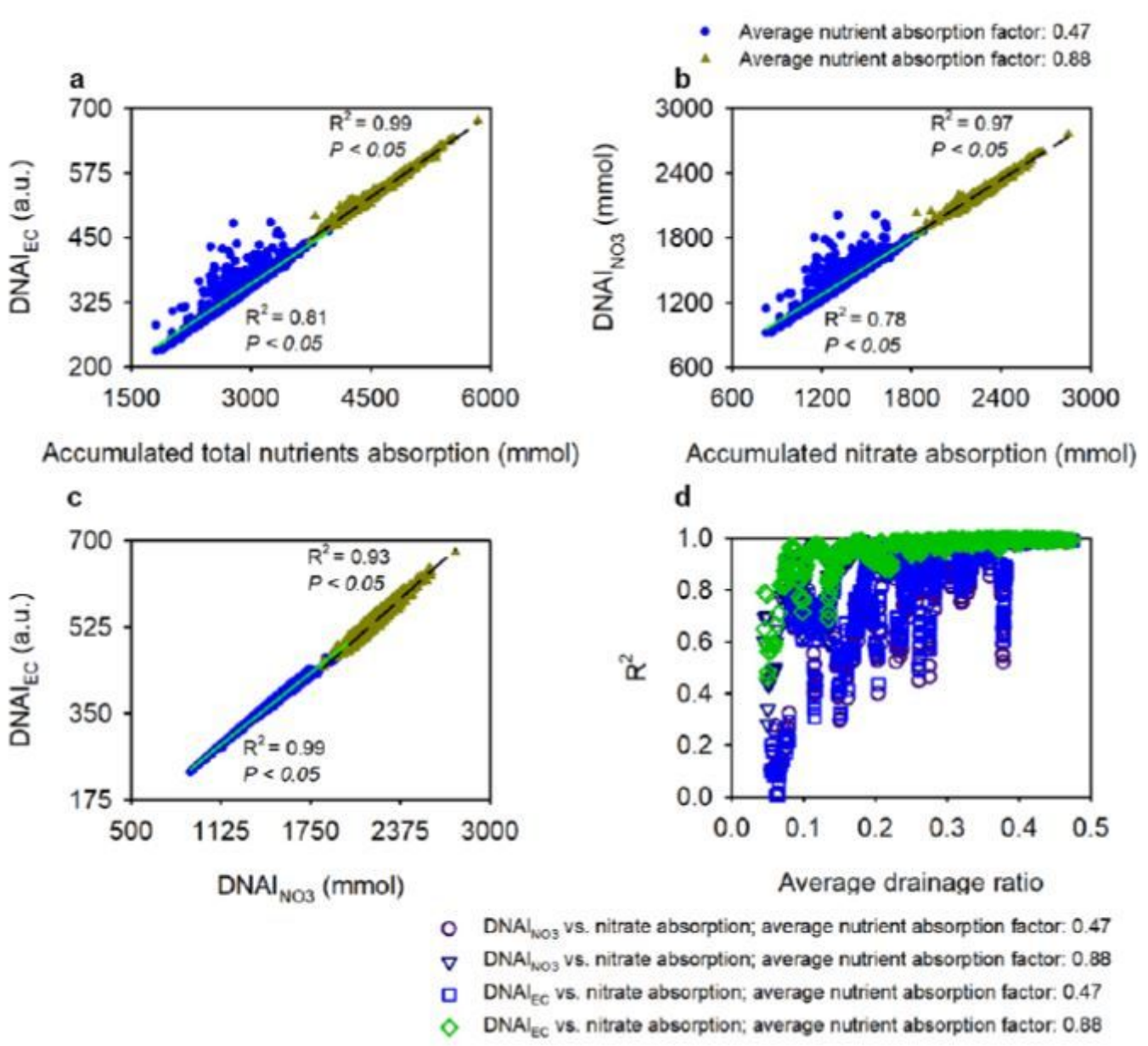

Figure 3

Correlations of DNAIEC (a) and DNAINO3 (b) with total nutrients and nitrate absorption under different average nutrient absorption factors in the simulation; (c) correlations between DNAIEC and DNAINO3 under different average nutrient absorption factors in the simulation; (d) changes in R2 between DNAIEC, NO3 and total nutrient or nitrate absorption according to average drainage ratio in the simulation (Number of simulations: 1000).

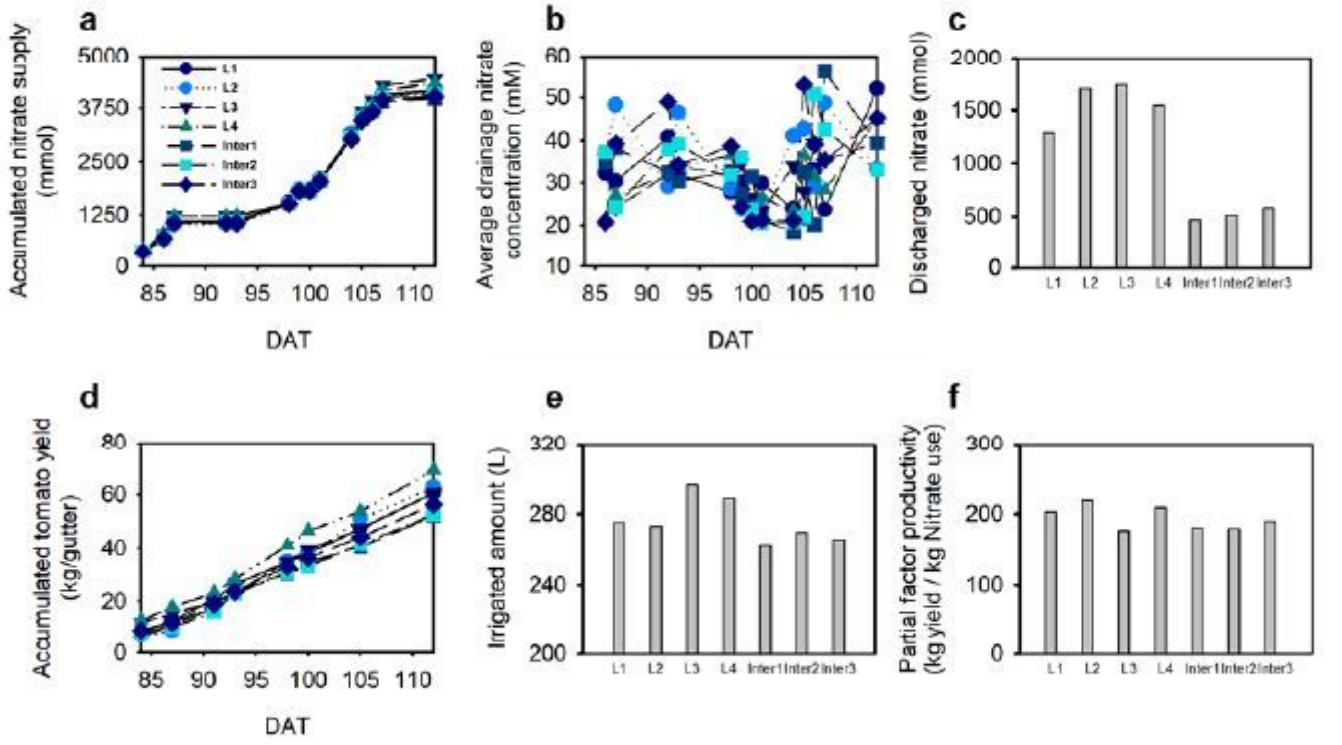

Figure 4

Accumulated nitrate supply (a), average nitrate concentration in drainage (b), accumulated discharged amount of nitrate (c), accumulated irrigation amount (d), accumulated tomato yield (e), and partial factor productivity (f) during the experimental period.

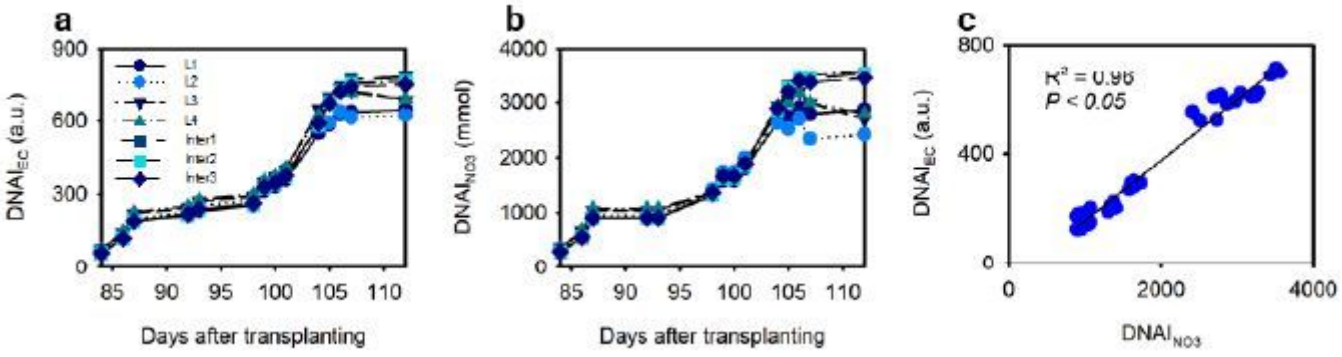

Figure 5

Changes in DNAIEC (a) and DNAINO3 (b) during the experimental period; (c) correlation between DNAIEC and DNAINO3.

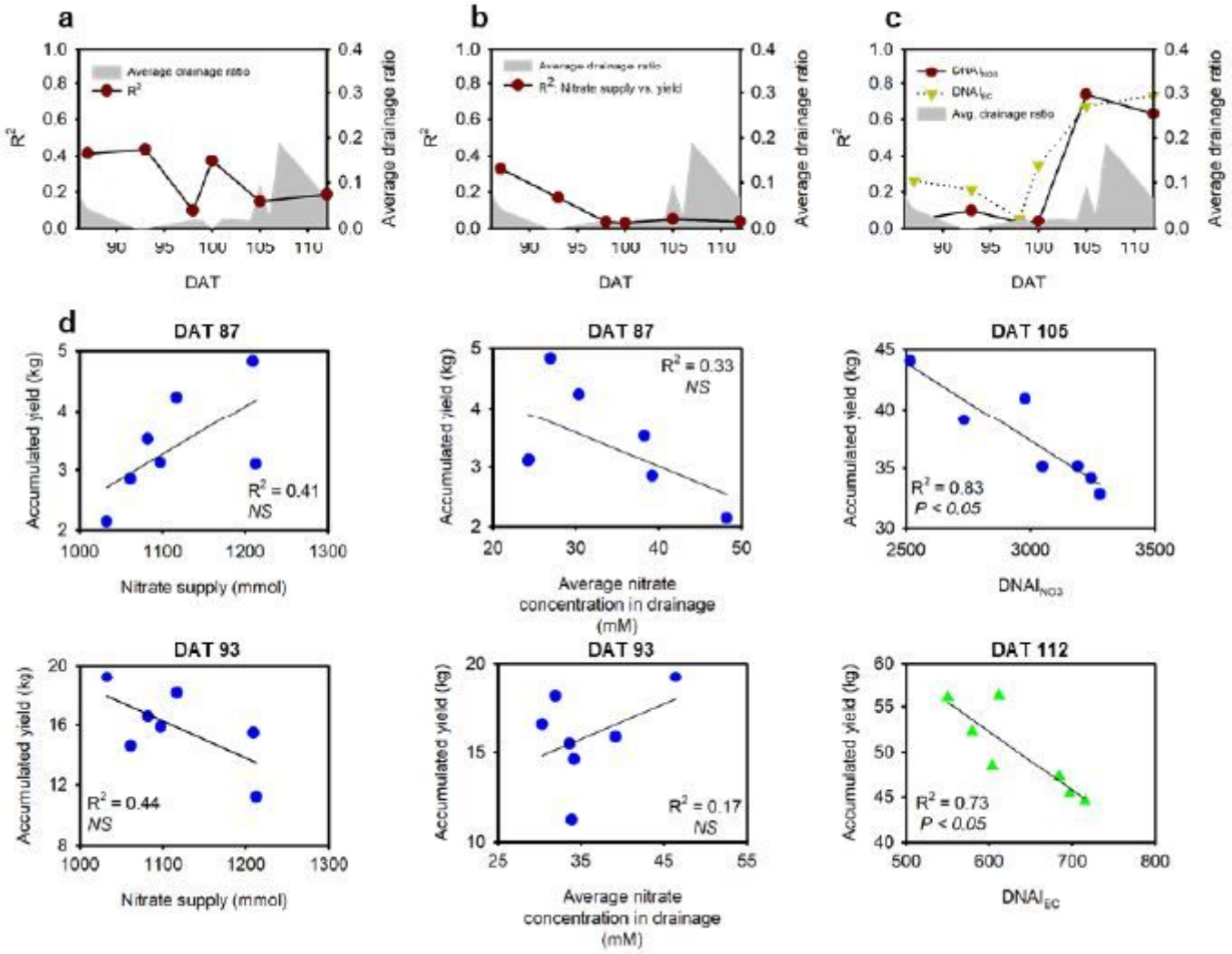

Figure 6

Changes in R2 values of the accumulated tomato yield with accumulated nitrate supply (a), average nitrate concentration in drainage (b), DNAIEC (c), and DNAINO3 (c); (d) representative correlations of accumulated tomato yield with accumulated nitrate supply, average nitrate concentration in drainage, DNAIEC, and DNAINO3.

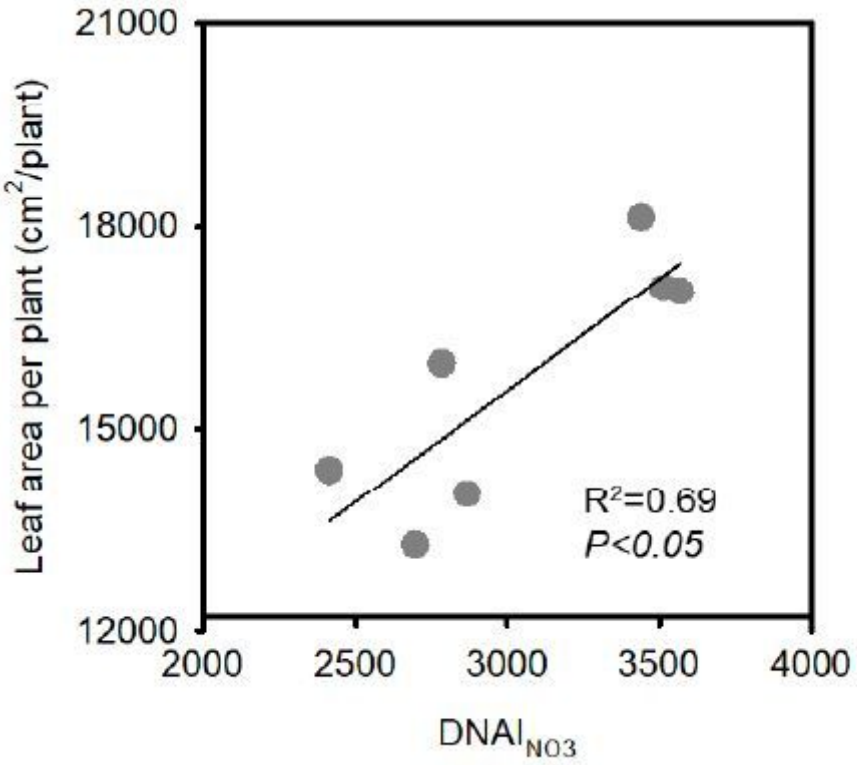

Figure 7

Correlation between non-destructively estimated tomato leaf area and DNAINO3 at the end of the experiment.

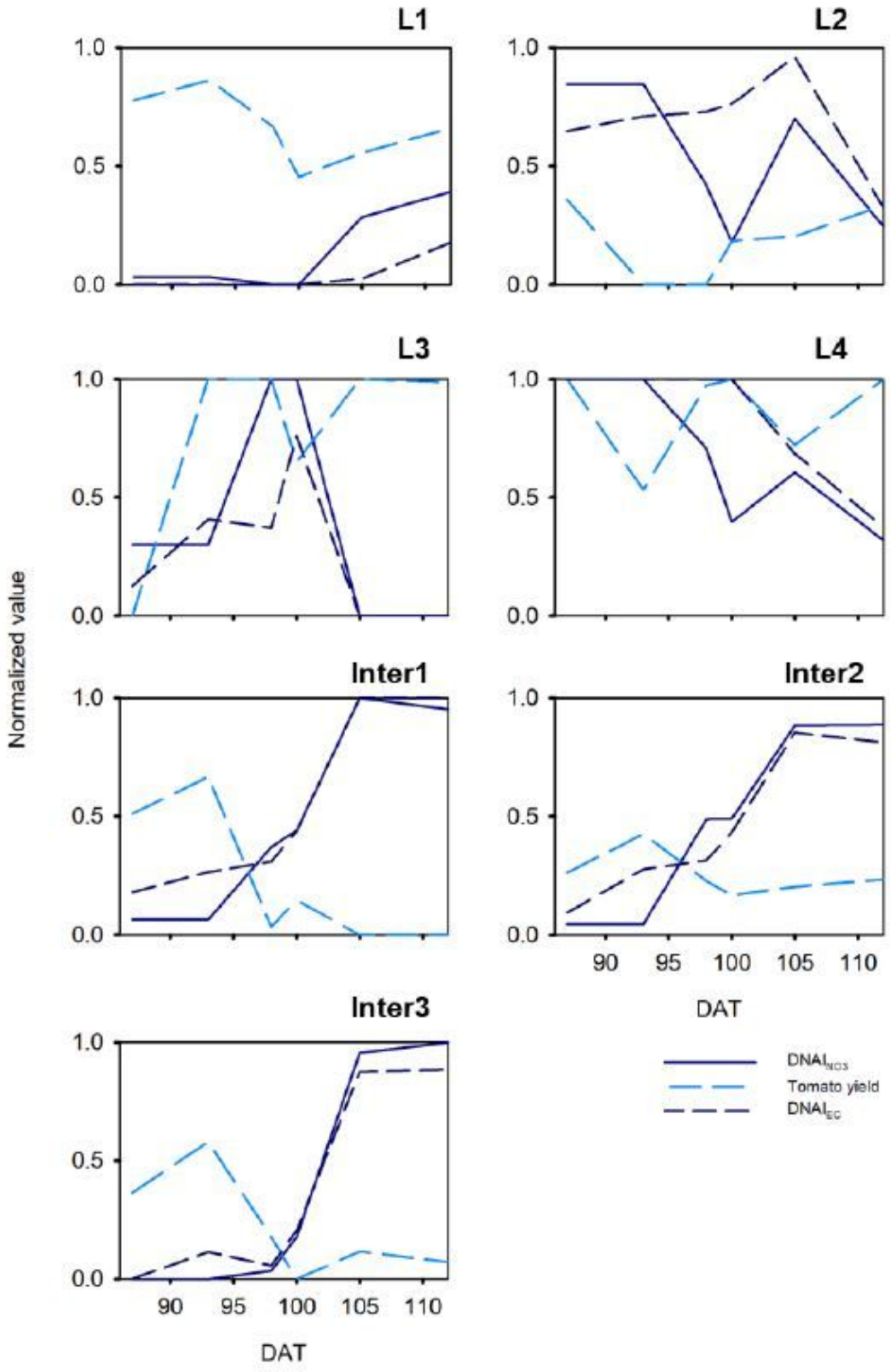

Figure 8

Changes in the normalized values of DNAIEC, DNAINO3, and accumulated tomato yield during the experimental period.